Experimental Study of SnO_2/SnO/Sn Thermochemical Systems for Solar Production of Hydrogen

Patrice Charvin and Stéphane Abanades
CNRS-PROMES (Processes, Materials, and Solar Energy Laboratory), 66120 Font Romeu, France

Florent Lemont
Commissariat à l'Energie Atomique, BP 17171, 30 207 Bagnols-sur-Cèze Cedex, France

Gilles Flamant
CNRS-PROMES (Processes, Materials, and Solar Energy Laboratory), 66120 Font Romeu, France

DOI 10.1002/aic.11584
Published online September 2, 2008 in Wiley InterScience (www.interscience.wiley.com).

A novel two-step thermochemical water-splitting cycle based on SnO_2/SnO is proposed from the detailed study of the whole tin oxide systems involving three redox pairs. The thermal reduction of tin(IV) oxide occurs in the temperature range 1400–1600°C following a zero order kinetic law of Arrhenius with an activation energy of 394.8 kJ mol^{-1} and a pre-exponential factor of 8.32 × 10^8 g s^{-1} at atmospheric pressure. The operating conditions that prevent gaseous stannous oxide (SnO) from recombining with O_2 are defined. The effect of a quenching device (water-cooled finger) is negligible whereas operation at low total pressure or low O_2 and SnO partial pressures leads to nearly pure SnO product. The comparison of SnO and metallic tin hydrolysis in a fixed bed reactor reveals a higher reaction rate in the case of SnO. Hydrolysis of these reduced compounds shows nearly complete conversion producing hydrogen by a solid/gas reaction proceeding at moderate temperature, thus easy to implement in a common reactor technology. © 2008 American Institute of Chemical Engineers *AIChE J,* 54: 2759–2767, 2008

Keywords: hydrogen, water-splitting, thermochemical cycles, tin oxides, solar concentrated energy

Introduction

Global warming caused by greenhouse gas emissions becomes one of the most worrisome issue for the future. The main source of CO_2 emissions is the result of fossil fuels combustion. Hydrogen fuel is proposed as an alternative carbon-free and sustainable energy carrier. Concentrated solar energy can supply process heat at high temperature for hydrogen production from water.

Direct thermal dissociation of water is impeded by the need of a high temperature heat source (>2500 K) and of an effective technique for separating H_2 and O_2. Thermochemical cycles consisting of a series of endothermic and exothermic reactions allow operation at much lower temperatures with the same global water decomposition reaction. Furthermore, water-splitting cycles bypass the H_2/O_2 separation

Correspondence concerning this article should be addressed to S. Abanades at abanades@promes.cnrs.fr.

problem and produce pure, affordable, and renewable solar hydrogen ready for use with virtually zero CO_2 emission. Therefore, water-splitting constitutes the ideal long term option for hydrogen production with tremendous environmental and economical impact because of the low value and abundance of its reactant. Electrolysis already employed to produce pure hydrogen, requires a first step of electricity production from solar thermal energy with a moderate energy efficiency (20–25%[1]) resulting in a global solar heat-to-hydrogen energy conversion efficiency of about 15–20%. Two or three-step thermochemical cycles generally based on metal oxide systems compete readily with electrolysis process because they exhibit higher theoretical energy conversions, thus offering the potential for efficient and large scale supply of H_2 as a clean energy carrier.[2]

Thermochemical cycles are composed of endothermic and exothermic reactions at different temperature levels, involving chemical intermediates recycled from one reaction to another. Then, the net reaction is only the dissociation of water to produce hydrogen and oxygen. A large number of intermediates and reaction routes are possible and compiled in reviews.[3–5] Next generation nuclear reactors (high temperature gas-cooled reactor–very high temperature reactor, HTGR–VHTR) may deliver thermal energy at 950°C whereas temperatures up to 2000°C can be obtained with concentrated solar energy. Then, the screening of promising cycles for solar energy coupling highlights the potential of two and three-step thermochemical cycles using metal oxides for producing hydrogen fuel.[2] The most simple two-step cycles proceed with the reduction of a metal oxide in an endothermic reaction at high temperature. This reduced oxide reacts with water at moderate temperature to regenerate the first oxide and to produce hydrogen:

$$MO_{ox} \rightarrow MO_{red} + 1/2\ O_2 \qquad (T > 1300^\circ C) \qquad (1)$$

$$MO_{red} + H_2O \rightarrow MO_{ox} + H_2 \qquad (T < 1000^\circ C) \qquad (2)$$

Several metal oxides (In_2O_3, MoO_2, WO_3, ZnO, SiO_2, Fe_3O_4) were proposed.[6,7] Recent developments mainly focused on ZnO/Zn[8–10] and Fe_3O_4/FeO[11–13] redox pairs to produce hydrogen in lab-scale reactors.

Currently, ZnO/Zn cycle is one of the most promising possible candidates for solar thermochemical production of hydrogen from water. It is known as the only cycle based on volatile metal oxide species, which means that the dissociation of solid ZnO produces gaseous species in the form of metallic zinc. The objective of this study is to propose and characterize an innovative two-step cycle based on the volatile SnO_2/SnO system.

A three-step thermochemical cycle involving SnO_2/Sn redox pair was patented in 1971,[14,15] but the so-called "Souriau cycle" was not demonstrated experimentally. The reactions proposed initially are the high-temperature reduction of stannic oxide (SnO_2) into stannous oxide (SnO) (Eq. 3), which disproportionates at 600°C into liquid metallic tin and stannic oxide (Eq. 4). Then, the recovery of metallic tin by phase separation is intended. The last exothermic step is the reaction of melted tin with water to produce hydrogen and to regenerate stannic oxide (Eq. 5).

$$2SnO_2 \rightarrow 2\ SnO(g) + O_2 \qquad (3)$$

$$2\ SnO \rightarrow 2\ Sn(1) + SnO_2 \qquad (4)$$

$$Sn(1) + 2H_2O \rightarrow 2\ SnO_2 + 2H_2 \qquad (5)$$

The earlier-mentioned cycle was experimentally examined in this study. The reactions proved to be experimentally possible but the following two main issues were raised: (1) the separation of metallic tin from SnO_2 was not feasible because the melted phase of Sn does not form and (2) Sn reactivity with water is weak resulting in a slow hydrolysis reaction. The tin-based redox process for hydrogen production was significantly improved by considering a novel two-step thermochemical cycle based on SnO_2 and SnO.[16] The first step is identical and corresponds to the high temperature thermal reduction of SnO_2 (Eq. 6), in which the heat input comes from concentrated solar energy. Dismutation of SnO into Sn and Sn(IV) is suppressed since this additional step does not generate oxygen, and then does not enhance hydrogen production. Therefore, a direct hydrolysis of SnO is considered in the second step to generate hydrogen (Eq. 7). This modification reduces the cycle complexity, when maintaining the same hydrogen productivity. The cycle is composed of solid–gas reactions only, which simplifies the separation of products.

$$SnO_2(s) \rightarrow SnO\ (g) + 1/2\ O_2 \qquad (6)$$

$$SnO\ (s) + H_2O \rightarrow SnO_2\ (s) + H_2 \qquad (7)$$

This article presents thermodynamics and experimental results for the solar thermal reduction of stannic oxide and hydrogen generation reaction. The operating conditions and stable species were predicted from thermodynamic equilibrium calculations for different tin-based systems. Then, the reactions were experimentally validated, temperature levels required for each reaction were investigated, reaction rates and chemical conversions were quantified.

Thermodynamics

The thermodynamic study is carried out with HSC Chemistry 5.11 software.[17] On the basis of the principle of Gibbs free energy minimization, calculations provide stable species and system composition at equilibrium for given operating conditions (temperature, pressure, and initial composition).

High-temperature reduction of stannic oxide

The reduction of stannic oxide generates gaseous products from a solid phase. The principle of Le Châtelier predicts an influence of total pressure P_{tot} and mole fraction of products x_i on the thermodynamic equilibrium constant K (Eq. 8) and then on the reaction temperature.

$$\Delta G^O = -RT\ \ln(K)\ \text{ with }\ K = \frac{p_{SnO} p_{O_2}^{0.5}}{P_0^{1.5}} = \frac{x_{SnO} x_{O_2}^{0.5} P_{tot}^{1.5}}{P_0^{1.5}} \qquad (8)$$

An increase of inert gas quantity results in a decrease of reaction temperature (Figure 1). The same effect can be observed with a reduction of the total pressure.

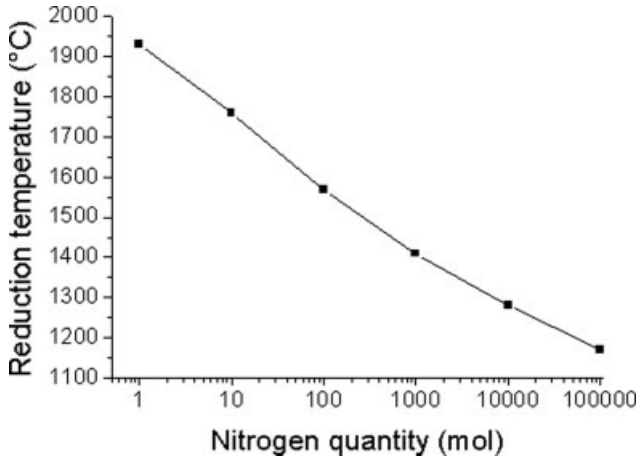

Figure 1. Temperature of complete SnO_2 reduction for different quantities of nitrogen in the feed (P = 100 kPa, SnO_2 = 1 mol).

These equilibrium calculations assume a closed system without any entrance and exit of compounds. An excess of nitrogen must be considered in thermodynamics to simulate a continuous flow of nitrogen that sweeps the produced gas species outside the reaction chamber.

Dismutation of SnO

The gaseous SnO is condensed during the cooling stage at a temperature of 1300°C (Figure 2, partial pressure of SnO equal to 1 kPa). Below this temperature, an equilibrium is observed between solid SnO and a mixture of Sn and SnO_2 that is produced by a dismutation reaction (Eq. 9) as previously observed for wustite.[11]

$$2SnO \leftrightarrow Sn + SnO_2 \qquad \Delta H^O = -16.2 \text{ kJ mol}^{-1} \qquad (9)$$

The formation of the mixture of Sn and SnO_2 is favored at low temperatures (Figure 2). The dismutation rate of SnO increases when temperature decreases according to thermodynamics. However, SnO remains stable at temperatures below 600°C (metastable state) due to kinetic limitations.

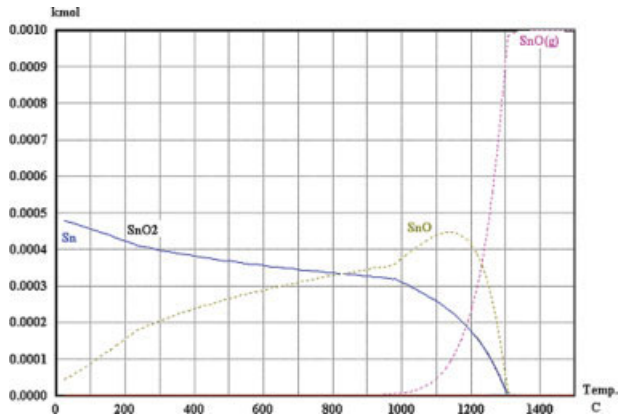

Figure 2. Temperature dependence of equilibrium composition for the dismutation of SnO (P = 100 kPa, N_2 = 100 mol, SnO = 1 mol).

[Color figure can be viewed in the online issue, which is available at www.interscience.wiley.com.]

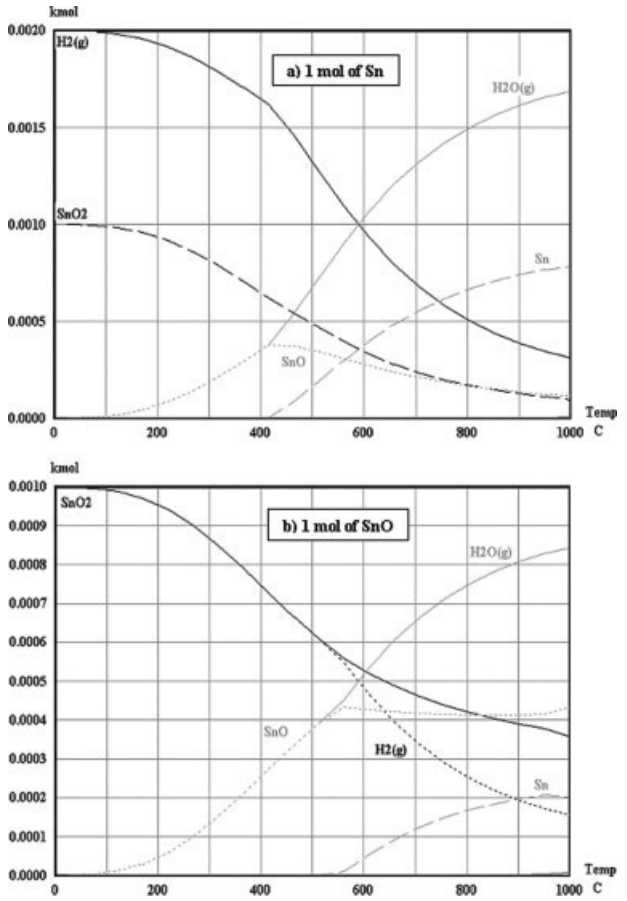

Figure 3. Equilibrium calculation of the Sn/O/H system for (a) 1 mol of Sn and (b) 1 mol of SnO (P = 100 kPa, N_2 = 100 mol).

Hydrolysis of reduced compounds

The oxidation of metallic tin into stannic oxide by steam is complete at low temperatures, but hydrogen production decreases when the temperature increases (Figure 3a). Small quantities of SnO are predicted in the temperature range 300–600°C. Thus, at these temperatures, the oxidation of metallic tin (Eq. 10) with water occurs whereas oxidation of SnO (Eq. 11) is not favorable.

$$2Sn + H_2O \rightarrow SnO + H_2 \qquad \Delta H^O = -38.9 \text{ kJ mol}^{-1} \qquad (10)$$

$$2SnO + H_2O \rightarrow SnO + H_2 \qquad \Delta H^O = -55.1 \text{ kJ mol}^{-1} \qquad (11)$$

Similarly to the case of tin, the simulation of SnO hydrolysis shows that the amount of hydrogen decreases with temperature (Figure 3b). The yield of hydrogen is about 50% at 600°C. According to thermodynamics, metallic tin and SnO show similar water-splitting performance with a yield of hydrolysis reaction higher than 50% below 600°C.

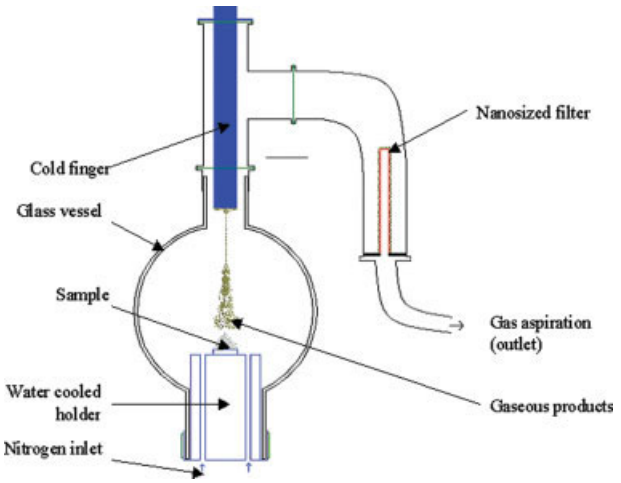

Figure 4. Experimental set-up used for the reduction of volatile metal oxides.

[Color figure can be viewed in the online issue, which is available at www.interscience.wiley.com.]

Reduction of Stannic Oxide

Experimental set-up and methods

Concentrated solar energy is employed as the heat source to study the thermal reduction of stannic oxide at high temperatures. Commercial powder of stannic oxide from PROLABO (purity: 99.9%) was compacted into pellets (8-mm diameter) under a pressure of 1 ton to obtain a flat surface. This sample (about 1 g) was placed on a water-cooled holder inserted in a glass vessel to control the atmosphere (Figure 4). A nitrogen flow used as inert gas was introduced in the vessel through the holder. A vacuum pump connected to the glass vessel maintained a circulation of the inert gas and allowed operations at reduced pressure. The continuous flow of inert carrier gas was used to cool down the gaseous products and carry them at the exit. A water-cooled refrigerant was set on the gas path to quench gas products and to condense SnO. A nanosized filter was placed after the quenching device to separate solid SnO particles from the gas.

Energy was provided by a solar furnace composed of a reflector (flat mirror) and a parabolic concentrator (1.5 m-diameter), which concentrates solar radiations at the focal point (gaussian distribution profile with a peak flux density of 16 MW m^{-2}). The sample was placed below the focal point to absorb a less concentrated solar flux. The gas release at the surface of the pellet indicates the beginning of the reduction reaction. The position of the sample with respect to the focal plane can be modified to increase the surface temperature and the reaction kinetic.

After a purge of oxygen from the experimental set up, the SnO_2 pellet was heated till the emission of a small quantity of gas from the top of the sample. The gas flow was laminar in the configuration of the experiment. The progressive growth of whiskers from the edge of the pellet was observed. The formation of such whiskers with a dendritic structure has already been reported in the case of zinc oxide reduction.[18] A rapid recombination of SnO and O_2 produced these whiskers composed of SnO_2 nanoparticles.

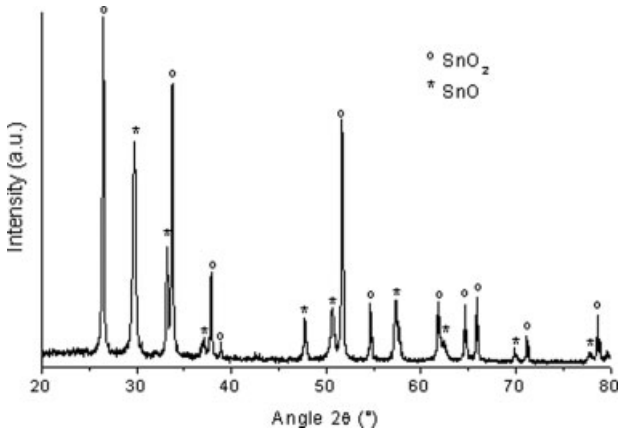

Figure 5. XRD pattern of a sample collected on the filter after SnO_2 solar processing.

At the end of the experiment, two deposits were collected on the cold finger and on the filter and analyzed by X-ray diffractometry (XRD). Results were similar for both samples (Figure 5) and showed a mixture of SnO and SnO_2 (SnO mass fraction: 28%). The mass fraction of SnO in the mixture was determined from the ratio between the intensity of major XRD peaks of the two species ($2\theta = 26.6^\circ$ for SnO_2 and $2\theta = 29.9^\circ$ for SnO). A calibration curve was established with standard mixtures prepared with a defined mass fraction of SnO (Figure 6). The relative uncertainty on the SnO mass fraction was estimated at 5%.

Stannic oxide observed in the product was not the result of a sublimation of the pellet because SnO_2 sublimes between 1800 and 1900°C,[19] which is somewhat higher than the reduction temperature. Thus, a recombination reaction between gaseous products (SnO and O_2) during the gas cooling must be considered as demonstrated for zinc.[20,21]

Effect of reduced compound addition

A reduced compound was introduced in the pellet of SnO_2 to fix oxygen in the solid phase and to validate the assumption of a recombination in the gas phase. Wustite (FeO) was mixed with SnO_2 before compaction. A gaseous product was

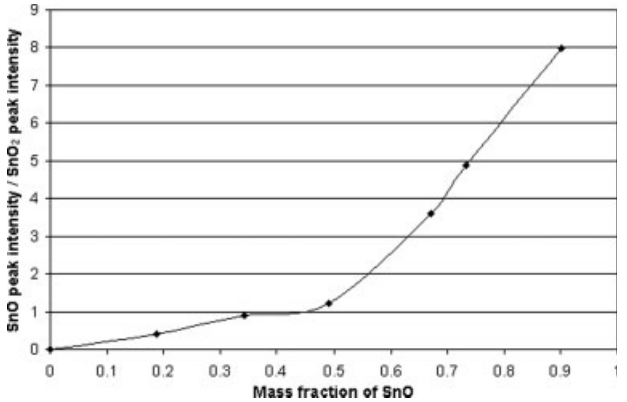

Figure 6. Calibration curve for mass fraction evaluation from XRD peaks intensities.

Table 1. Results of SnO_2 Solar Reduction for Different Configurations of Gas Quenching, Pressures, and N_2 Flow-Rates

No.	Cold Finger Distance (cm)	N_2 Flow-Rate (L min^{-1})	Total Pressure (kPa)	Reduction Rate (μmol min^{-1})	SnO Content (% in Mass)
1	10	1.3	85	na	20
2	6	1.3	85	na	40
3	4	1.3	85	na	54
4	4	1.3	85	0.6	100
5	4	1.3	85	1.7	95
6	4	1.3	85	20	63
7	4	1.3	85	79	43
8	4	1.3	85	126	33
9	4	0.34	2	100	90
10	4	0.34	10	100	63
11	4	0.34	30	100	18
12	4	0.34	60	100	15

emitted during sample heating in the same range of temperature (1400–1600°C) than for pure SnO_2. The water-cooled refrigerant was removed from the set up to reduce the quenching rate.

XRD analysis revealed SnO as the only compound in the filter deposit. The absence of SnO_2 means that the only gas product emitted by the pellet was the reduced oxide SnO. The addition of wustite in the pellet trapped the oxygen generated by the reduction of SnO_2. Then, only the gaseous SnO was released, and it was not oxidized after its formation. This method was used to produce pure samples of SnO, which were used for studying the hydrolysis reaction. However, the use of wustite as a reducing agent can not be considered in the thermochemical cycle. The recombination reaction must be limited to produce pure SnO without the use of any chemical reactant.

Recombination limitation

An increase of the quenching rate was achieved by approaching the cold finger from the top of the pellet to cool down the gas products as quickly as possible. A minimum distance of 3 cm between the cold finger and the pellet was imposed to limit the shadowing caused by the cold finger. The recombination reaction was slightly reduced to reach a SnO yield of 54% for the closest position of the cold finger (Table 1, no. 1–3).

The reduction was carried out for different surface temperatures and then different reaction rates. The deposit exhibited the highest mass fractions of SnO for experiments with a slow reduction rate (Table 1, no. 4–8). In these cases, the flow-rate of products (SnO and O_2) was reduced whereas the inert gas flow-rate was constant (F_{N2} = 1.3 L min^{-1}). Then, the O_2 partial pressure was decreased, which inhibited the recombination.

A total pressure reduction also modified the equilibrium constant between SnO and SnO_2, which increased SnO content in the filter deposit. The effect of pressure was investigated (Table 1, no. 9–12). The dilution with N_2 was fixed by maintaining constant both the nitrogen flow-rate and the reduction rate (N_2/SnO ratio of about 150). A nearly complete reduction (>90%) was obtained for a total pressure of 2 kPa with a constant nitrogen flow-rate of 0.34 L min^{-1} (Table 1, no. 9). At low pressure, the position of the cold finger and the nitrogen flow-rate had a weak influence on the yield of SnO. Thus, the amount of inert gas consumed in a solar process would be sharply lowered if the reduction reaction was carried out at low pressure.

Products characterization

The deposit collected on the filter came from the condensation of SnO(g) during gas cooling. This process produced very small SnO particles with a diameter smaller than a micron. These nanoparticles were responsible for the widening of the diffraction peaks obtained by X-ray analysis. The Sherrer formula (Eq. 12) was used to evaluate the average crystallite size from the full width at half maximum of XRD peaks. A mean diameter of about 50 nm was obtained for samples treated in different conditions of quenching.

$$d = \frac{0.9\lambda}{L\ \cos\theta} \tag{12}$$

where d is the average diameter of crystallites; λ is the wavelength of the X-ray used (λ = 0.154 nm); L is the full width at half maximum corrected with instrumental parameters (rad); and θ is the angle of the diffraction peak (rad).

Scanning electron microscopy revealed aggregates of nanoparticles. The average size of primary particles was between 50 and 100 nm. Darts and spheres were the two different types of particles observed. The number of darts seemed to decrease for samples with a high content of SnO.

Reduction kinetics

Thermogravimetric analysis (TGA) was performed to evaluate the reaction order and kinetic parameters. The device (SETARAM) was composed of two furnaces in parallel with alumina crucibles. It was used to measure the mass loss as a function of temperature. A program composed of several temperature plateau separated by rapid temperature increase was implemented (Figure 7). Thus, the reaction rate was determined at isothermal conditions. Three orders of the reaction kinetic (order 0, 1, and 2) were considered in Eq. 13 for a temperature of 1450°C and a pressure of 1 kPa. After integration of Eq. 13, a single reaction order (order 0) best fitted the rate of mass loss (Figure 8).

$$\frac{dm}{dt} = k(T)m^n \tag{13}$$

where m is the mass of the sample (g); $k(T)$ is the kinetic constant at temperature T; n is the order of the reaction.

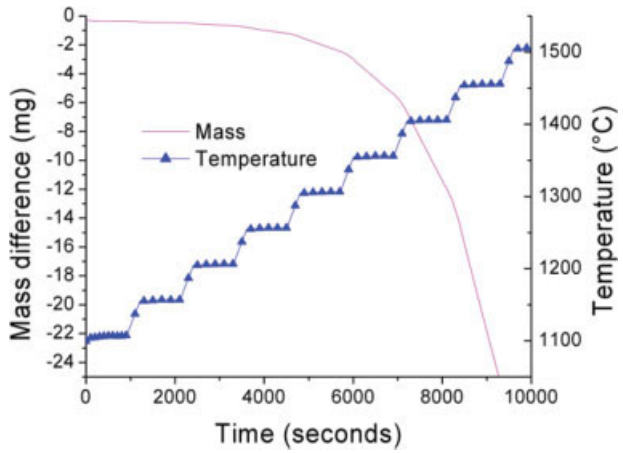

Figure 7. Temperature program and mass evolution during a TGA experiment with SnO_2.

[Color figure can be viewed in the online issue, which is available at www.interscience.wiley.com.]

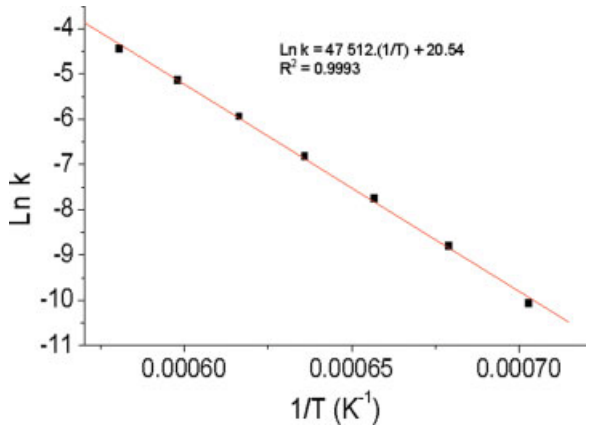

Figure 9. Determination of the kinetic parameters (atmospheric pressure).

[Color figure can be viewed in the online issue, which is available at www.interscience.wiley.com.]

Assuming a zero order reaction, mass slopes gave values of the kinetic constant $k(T)$ for the temperature of the plateau. Figure 9 plotted for experiments at atmospheric pressure shows a linear evolution of ln $k(T)$ vs. $1/T$, which leads to an activation energy of 394.8 kJ mol^{-1} and a pre-exponential factor of 8.32×10^8 g s^{-1} assuming an Arrhenius kinetic expression. At low pressure, the reaction kinetics was improved with a pre-exponential factor of 1.55×10^9 g s^{-1} at $P = 10$ kPa and 4.81×10^9 g s^{-1} at $P = 1$ kPa. For a given kinetic rate, operation temperature was thus reduced (about 150 K) at $P = 1$ kPa (Figure 10). Similar thermogravimetric isothermal experiments were performed in the case of ZnO for dissociation rate comparison. The reduction of SnO_2 required higher temperatures (about 80 K) to obtain the same kinetic rates than ZnO reduction.

In conclusion, a low pressure operation enhanced the reaction kinetics for a given temperature or lowered the operation temperature for a given reaction rate. Furthermore, recombination of products was limited at low pressure enabling a high content of SnO in the product.

Steam Hydrolysis of Reduced Compounds

Three-step Souriau cycle

Dismutation. A pure SnO sample reduced at the focus of a solar furnace was introduced in a quartz test tube. Nitrogen was injected in the test tube to sweep oxygen out. A type-K thermocouple measured the temperature of the powder inside the tube. The sample was then heated at 600°C during 15 min. A gray powder was obtained after the experiment. No sign of a liquid phase due to the melting of metallic tin as suggested in[14] was noticed. Metallic tin and SnO_2 were identified as the only products by XRD analysis (Figure 11). Thus, the dismutation reaction was complete because no peak of SnO was detected. The nanoparticles were saved

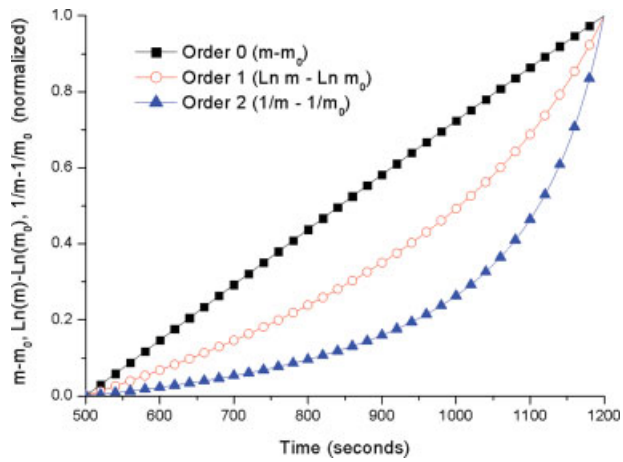

Figure 8. Investigation of the order of the reduction reaction ($T = 1450$°C, $P = 1$ kPa).

[Color figure can be viewed in the online issue, which is available at www.interscience.wiley.com.]

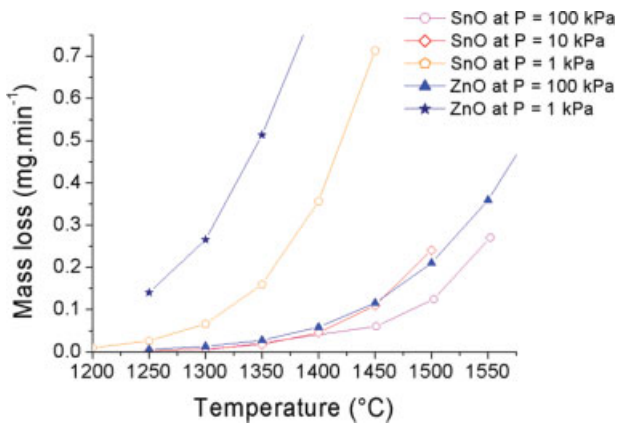

Figure 10. Evolution of the kinetic rate vs. temperature for SnO_2 and ZnO reduction at different pressures.

[Color figure can be viewed in the online issue, which is available at www.interscience.wiley.com.]

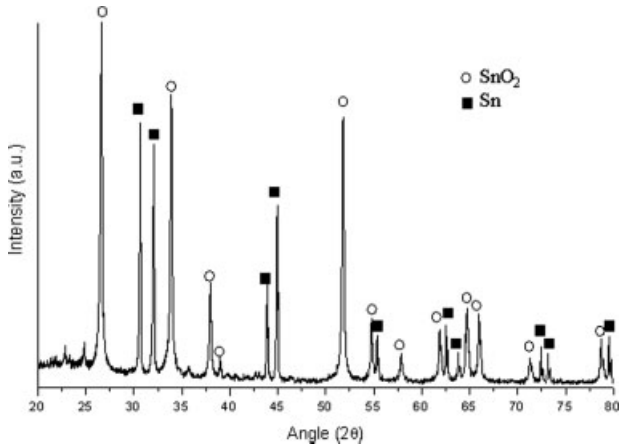

Figure 11. XRD pattern of the sample of SnO heated 15 min. at 600°C in a nitrogen atmosphere.

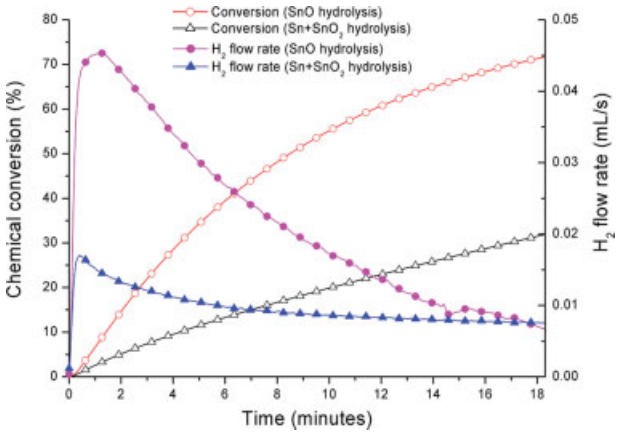

Figure 13. Chemical conversion and H_2 production for SnO_2 + Sn and SnO hydrolysis at 525°C.

[Color figure can be viewed in the online issue, which is available at www.interscience.wiley.com.]

(particle diameter unchanged) thanks to the absence of tin melting during the reaction.

Tin hydrolysis. The stoichiometric mixture of Sn and SnO_2 obtained after the dismutation reaction (Eq. 9) was hydrolyzed in a fixed bed reactor heated by an electrical furnace at 525°C. Steam was generated in a first upstream furnace and carried out by an argon flow (F_{Ar} = 0.18 L min^{-1}). It then passed through the fixed bed of solid mixture (0.2 g) to react with Sn heated at 525°C (Figure 12). The amount of produced hydrogen was measured continuously by a catharometer (ARELCO Catarc 10P, detection limit: 100 ppm, precision: 1% of full scale) at the reactor outlet.

Hydrogen production started few seconds after water introduction to reach a maximum flow-rate of 5 mL min^{-1} per gram of mixture Sn + SnO_2. Then, the measurement signal of H_2 decreased slowly until the end of the experiment. The chemical conversion, defined as the ratio between the total mole of hydrogen produced to the initial mole of reactant in the sample, was about 32% after 18 min and 45% after 30 min (Figure 13). The reaction rate was slow at 525°C. The chemical conversion increased regularly to exceed 70% after 1 h. Thus, no passivation phenomenon occurred at the surface of nanoparticles whereas this unfavorable issue was reported for zinc or wustite hydrolysis.[11,13]

In conclusion, SnO dismutation and tin hydrolysis reactions were nearly complete with a rapid kinetic for the first reaction and a slow reaction rate for the second one. However, the separation of SnO_2 and Sn after dismutation, as proposed in Ref. 14 is impractical because the stoichiometric SnO_2/Sn mixture remains in the solid state at 600°C.

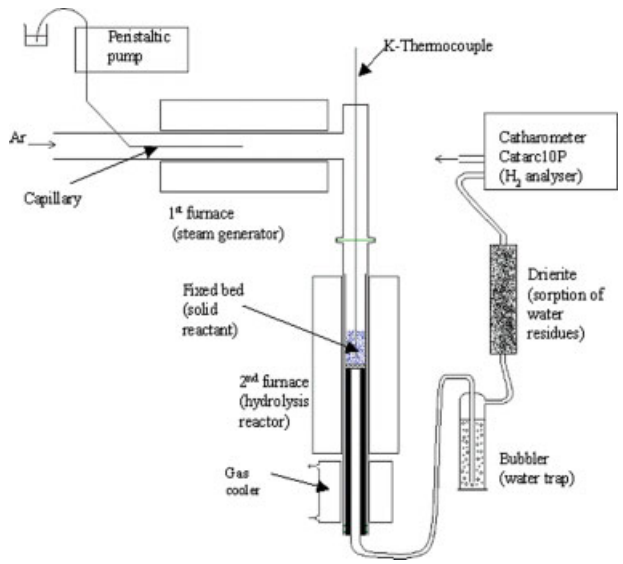

Figure 12. Experimental set-up used for water-splitting reactions.

[Color figure can be viewed in the online issue, which is available at www.interscience.wiley.com.]

Novel two-step SnO_2/SnO cycle: SnO hydrolysis

The direct hydrolysis of SnO was carried out in the experimental set-up previously described and used for Sn hydrolysis (Figure 12). A temperature of 525°C was selected for the first experiment to compare kinetic rates and chemical conversions. The introduction of water steam through a 0.2 g sample of pure SnO induced an increase of the H_2 concentration measured by the catharometer few seconds later. The production of hydrogen rapidly reached a maximum value of 13.6 mL min^{-1} per gram of SnO. The chemical conversion was higher than 71% after 18 min of hydrolysis (Figure 13). Thus, SnO hydrolysis exhibits a better kinetic rate and a higher conversion than metallic tin hydrolysis although its oxidation degree is higher.

In a two-step process, the use of wustite to produce pure SnO is prohibited during the reduction reaction. Commonly, the product of the high temperature step contains a small fraction of SnO_2 due to the partial recombination of products during the quenching. Thus, mixtures of SnO/SnO_2 produced from solar SnO_2 reduction were hydrolyzed to study the possible effect of SnO_2. The kinetic rates obtained at 525°C for mixtures of SnO and SnO_2 were similar to those observed for pure SnO samples (Table 2). The results concerning the

Table 2. Results of SnO Hydrolysis

No.	SnO Purity in the Sample (% in Mass)	Reaction Temperature (°C)	Maximum H_2 Flow-Rate (mL min^{-1} g^{-1}_{SnO})	Duration of Experiment (min)	$\eta_{experimental}$ (%)	$\eta_{hydrolysis}$ (%)
1	100	480	12.6	28	71	71
2	100	525	13.6	23	73	73
3	100	470	9	31	83	83
4	86	525	16.8	26	75.7	88
5	75	525	14.4	30	72.7	97
6	72	525	13.8	25	63.4	88
7	90	525	12.2	40	85.5	95
8	68	625	50.4	9	57.1	84

chemical conversions varied from an experiment to another due to calculation assumptions. In a first step, calculations were achieved for a pure sample of SnO. As the purity in SnO was different in each sample due to recombination, a correction was then applied to the conversion (Eq. 14) to take into account the initial content of SnO in the sample.

$$\eta_{hydrolysis} = \frac{\eta_{experimental}}{x_{SnO}} \tag{14}$$

where $\eta_{hydrolysis}$ is the chemical conversion of the hydrolysis reaction; $\eta_{experimental}$ is the chemical conversion calculated for a pure sample of SnO; and x_{SnO} is the initial content of SnO in the sample.

The chemical conversions of the hydrolysis were higher than 80% at 525°C (Table 2). The small size of particles produced in the high-temperature step (diameter below 100 nm) induced a large surface area available for the reaction, which explained the absence or negligible effect of passivation. However, the time duration necessary for a complete reaction (30 min) was similar to that reported for the hydrolysis of large particles of wustite (30 $\mu m < d_p < 50$ μm).[13]

The influence of temperature on the chemical conversion was investigated (Figure 14). Reaction temperature was increased up to 625°C, which improved the initial reaction rate. At this temperature, the hydrolysis of SnO was theoretically in competition with the dismutation reaction. The latter might produce metallic tin featuring a slow hydrolysis kinetic rate but this parasitic reaction was not observed. Indeed, the maximum H_2 production rate was increased fourfold with respect to experiments at 525°C (Table 2), whereas the final conversion was kept unchanged (above 80%). Thus, the hydrolysis of SnO over 600°C is preferable to increase reaction kinetics and to achieve the hydrolysis reaction in less than 10 min.

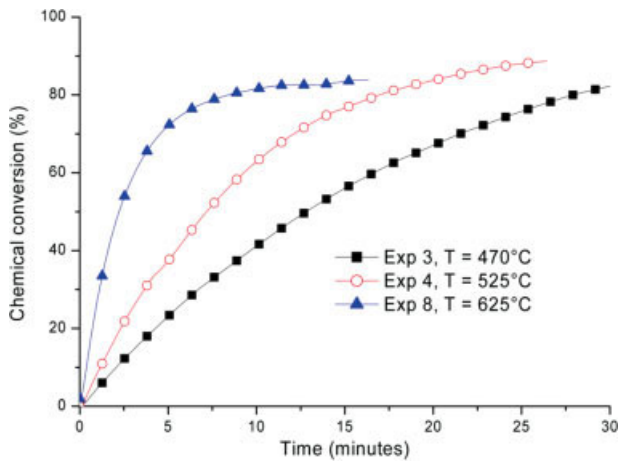

Figure 14. Chemical conversion of SnO hydrolysis at different temperatures.

[Color figure can be viewed in the online issue, which is available at www.interscience.wiley.com.]

The relative reaction rate can be estimated as the rate of conversion increase during the first few minutes of isothermal hydrolysis experiments (Figure 14). It can be obtained for each temperature from the slope of the chemical conversion increase at the starting time. A logarithmic plot of these data vs. $1/RT$ allows estimating the apparent activation energy of SnO hydrolysis as 67.4 kJ mol^{-1} (linear regression, $R^2 = 0.999$).

Conclusion

The experimental study of thermal reduction and hydrolysis reactions demonstrated two possible pathways to produce hydrogen from the SnO_2/SnO/Sn redox systems. The first three-step cycle ("Souriau" cycle) consists of a thermal reduction of SnO_2 into SnO at high temperature, a dismutation of SnO complete after 15 min of heating at 600°C, and an hydrolysis of metallic tin in the mixture (Sn + SnO_2). Although the nearly complete hydrolysis was observed due to nanoparticle size, the reaction kinetics was very slow and the reaction duration was estimated at about 1 h (final conversion above 70%). In addition, the separation of Sn and SnO_2 after dismutation is not achievable by simple phase separation because the melting of metallic tin does not occur at 600°C in the presence of a stoichiometric Sn–SnO_2 mixture.

A novel two-step cycle based on the SnO_2/SnO redox pair was then proposed and investigated. The kinetic parameters of SnO_2 reduction were determined by isothermal TGA for different pressures (E_a = 394.8 kJ mol^{-1}, k_0 = 8.32×10^8 g s^{-1} at atmospheric pressure). For a given reaction temperature, a pressure decrease enhanced the kinetic rate of the solid–gas dissociation reaction. The reduction conditions and gas quenching were optimized to limit the recombination of products in the gas phase. A low partial pressure of oxygen obtained from either a total pressure reduction or an introduction of inert gas, was more efficient to reduce the recombination than an improvement of the quenching rate. The hydrolysis of SnO nanoparticles (50–100 nm) was nearly complete thanks to the large surface area available for the reaction with steam. An apparent activation energy of

67.4 kJ mol^{-1} was obtained. A reaction temperature in the range 550–625°C favored the reaction kinetics. SnO_2/SnO thermochemical system was thus demonstrated to be a promising candidate cycle for solar production of hydrogen.

Acknowledgments

This study was funded by the Department of Engineering Science of CNRS. Authors gratefully acknowledge Roger GARCIA for construction of the solar experimental reactor and Eric BECHE for XRD analysis.

Literature Cited

1. Romero M, Buck R, Pacheco JE. An update on solar central receiver systems, projects, and technologies. *J Solar Energ Eng*. 2002;124: 98–108.
2. Abanades S, Charvin P, Flamant G, Neveu P. Screening of water-splitting thermochemical cycles potentially attractive for hydrogen production by concentrated solar energy. *Energy*. 2006;31:2469–2486.
3. Bamberger CE. Hydrogen production from water by thermochemical cycles; a 1977 update. *Cryogenics*. 1978;18:170–183.
4. Beghi GE. Review of thermochemical hydrogen production. *Int J Hydrogen Energ*. 1981;6:555–566.
5. Yalçin S. A review of nuclear hydrogen production. *Int J Hydrogen Energ*. 1989;18:551–561.
6. Bilgen E, Bilgen C. Solar hydrogen production using two-step thermochemical cycles. *Int J Hydrogen Energ*. 1982;7:637–644.
7. Nakamura T. Hydrogen production from water utilizing solar heat at high temperature. *Solar Energ*. 1977;19:467–475.
8. Möller S, Palumbo R. Solar thermal decomposition kinetics of ZnO in the temperature range 1950–2400 K. *Chem Eng Sci*. 2001;56: 4505–4515.
9. Steinfeld A. Solar hydrogen production via a two-step water-splitting thermochemical cycle based on Zn/ZnO redox reactions. *Int J Hydrogen Energ*. 2002;27:611–619.
10. Wegner K, Ly HC, Weiss RJ, Pratsinis SE, Steinfeld A. In situ formation and hydrolysis of Zn nanoparticles for H_2 production by the 2-step ZnO/Zn water-splitting thermochemical cycle. *Int J Hydrogen Energ*. 2006;31:55–61.
11. Weidenkaff A, Nüesch P, Wokaun A, Reller A. Mechanistic studies of the water-splitting reaction for producing solar hydrogen. *Solid States Ionics*. 1997;101–103:915–922.
12. Steinfeld A, Sanders S, Palumbo R. Design aspects of solar thermochemical engineering-a case study: two-step water-splitting cycle using the Fe_3O_4/FeO redox system. *Solar Energ*. 1999;65:43–53.
13. Charvin P, Abanades S, Flamant G, Neveu P, Lemort F. Two-step water-splitting thermochemical cycle based on iron oxide redox pair for solar hydrogen production. *Energy*. 2007;32:1124–1133.
14. Souriau D. Process and set-up for thermal energy use at high temperature, in particular nuclear energy. Gaz de France, Patent no. 2135421, 1971.
15. Souriau D. Method and device for the use of high temperature heat energy, in particular of nuclear energy. Gaz de France, Patent no. 3761352, 1972.
16. Abanades S, Charvin P, Flamant G, Lemort F. Hydrogen production by water-splitting with SnO using the SnO_2/SnO redox pair in a series of thermochemical reactions. CNRS/CEA, Patent no.0753533, PCT/FR2008/050295, 2007.
17. Roine A. *HSC Chemistry 5.11*. Pori, Finland: Outokumpu Research Oy, 2002.
18. Weidenkaff A, Reller AW, Wokaun A, Steinfeld A. Thermogravimetric analysis of the ZnO/Zn water splitting cycle. *Thermochim Acta*. 2000;359:69–75.
19. Weast RC, Astle MJ. *CRC handbook of chemistry and physics*, 63rd ed. Boca Raton, FL: CRC Press, 1982.
20. Weidenkaff A, Steinfeld A, Wokaun A, Auer PO, Eichler B, Reller A. Direct solar thermal dissociation of zinc oxide: condensation and crystallisation of zinc in the presence of oxygen. *Solar Energ*. 1999; 65:59–69.
21. Keunecke M, Meier A, Palumbo R. Solar thermal decomposition of zinc oxide: an initial investigation of the recombination reaction in the temperature range 1100–1250 K. *Chem Eng Sci*. 2004;59:2695–2704.

Manuscript received Mar. 12, 2008, and revision received May 23 2008.